Numer Algor (2018) 78:1217–1231
https://doi.org/10.1007/s11075-017-0420-z

ORIGINAL PAPER

On the limit cycles, period-doubling, and quasi-periodic solutions of the forced Van der Pol-Duffing oscillator

Jifeng Cui[1] · Wenyu Zhang[1] · Zeng Liu[2] · Jianglong Sun[2,3,4]

Received: 3 July 2017 / Accepted: 18 September 2017 / Published online: 26 September 2017

Abstract In this paper, the limit cycles, period-doubling, and quasi-periodic solutions of the forced Van der Pol oscillator and the forced Van der Pol-Duffing oscillator are studied by combining the homotopy analysis method (HAM) with the multi-scale method analytically. Comparisons of the obtained solutions and numerical results show that this method is effective and convenient even when t is large enough, and the convergence of the approximate solutions is discussed by the so-called discrete square residual error. This method is a capable tool for solving this kind of nonlinear problems.

✉ Jianglong Sun
sundapao@126.com

Jifeng Cui
cjf@imut.edu.cn

Wenyu Zhang
2867420544@qq.com

Zeng Liu
z_liu@hust.edu.cn

[1] College of Science, Inner Mongolia University of Technology, Hohhot 010051, China

[2] School of Naval Architecture and Ocean Engineering, Huazhong University of Science and Technology, Wuhan 430074, China

[3] Hubei Key Laboratory of Naval Architecture and Ocean Engineering Hydrodynamics, Huazhong University of Science and Technology, Wuhan 430074, China

[4] Collaborative Innovation Center for Advanced Ship and Deep-Sea Exploration, Shanghai 200240, China

Keywords Van der Pol oscillator · Van der Pol-Duffing oscillator · Limit cycles · Period-doubling · Quasi-periodic · HAM

1 Introduction

Research in nonlinear oscillatory systems has a long history [1–4]. As the typical examples, the Van der Pol equation and the Van der Pol-Duffing equation have a long history of being used in both the physical and biological sciences. For instance, in biology, Fitzhugh [5] and Nagumo [6] extended the equations in a planar field as a model for action potentials of neurons. The equations have also been utilised in seismology to model the two plates in a geological fault [7], and in studies of phonation to model the right and left vocal fold oscillators [8]. In addition to the right applications of the physical model, the jump phenomena, limit cycles, period-doubling solutions, and quasi-periodic solutions of the forced Van der Pol oscillator and the forced Van der Pol-Duffing oscillator have been paid attention and researched wildly these years [9, 10]. It is worth mentioning that the Polish scientist Szemplinska-Stupnicka studied the properties of the Van der Pol-Duffing system using the numerical simulation, integro-differential methods, spectral analysis method, and Neimark-Sacker bifurcation theory, and concluded that "It is known that in the literature on nonlinear oscillations and on approximate analytical methods one can ***hardly*** find a clear indication as to how to determine an almost-periodic solution in the Van der Pol-Duffing system" [11]. Fortunately, in the latest studies, some good results about quasi-periodic solutions of the forced Van der Pol-Duffing oscillator were obtained by Shukla et al. using the homotopy analysis method (HAM) [12]. However, Fig. 1 illustrates that the results obtained by Shukla et al. are invalid when t is large ($t \in [990, 1000]$). In fact, their results are valid only when t is small, such as $t \in [0, 100]$. So, a new method put forward in this paper to correct Shukla's results is necessary.

In this paper, we investigate the limit cycles and quasi-periodic solutions of the forced Van der Pol-Duffing oscillator in the form

$$u'' - \mu(1 - u^2)u' + \alpha u + \beta u^3 = g\cos(\omega_f t) \tag{1}$$

subject to the initial conditions

$$u(0) = a, \quad u'(0) = 0 \tag{2}$$

where the prime denotes the differential with respect to the time t, ω_f is the frequency of the external force $F = g\cos(\omega_f t)$, and $\mu > 0, \alpha, \beta, g$ are constant physical parameters, and a is the amplitude of the oscillator which is unknown, respectively.

Particular cases of (1) namely, the Van der Pol oscillator ($\alpha = 1, \beta = 0, g = 0$) and the Van der Pol-Duffing oscillator ($\alpha = 1, g = 0$) have been solved analytically in [13] and [14], respectively by Chen and Liu. They have used the HAM to obtain closed form limit cycle solutions without external forcing. We know that a limit cycle solution depends on two physical quantities, one is the amplitude of the oscillator, and the other is its frequency. Approximately, analytical solutions for the forced Van

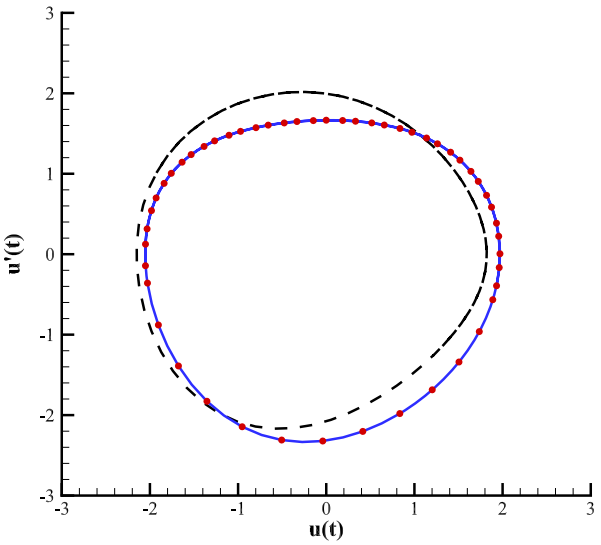

Fig. 1 Comparison of the $u - \dot{u}$ plane projection among the 15th-order approx. of our solution, 15th-order approx. of Shukla's paper and the numerical results when $t \in [990, 1000]$ in the case of $\mu = \frac{1}{10}, \beta = 0, \alpha = 1, g = \frac{1}{2}, w_f = 2$. Solid: 15th-order approx. of our solution; Dashed: 15th-order approx. of Shukla's paper; Filled circle: numerical results

der Pol-Duffing oscillator (1) have been reported by Kimiaeifar et al. [15], but they have not discussed limit cycle behavior.

2 Homotopy analysis method

As mentioned by Kartashova [16], "physical classification of PDEs is based not on the form of equations, but on the form of solutions." So, let us consider here such a "stationary" solution of $u(t)$ that can be expressed in the form

$$u(t) = \sum_{m=0}^{+\infty} \sum_{n=-\infty}^{+\infty} a_{m,n} \cos(m\omega t + n\omega_f t) + b_{m,n} \sin(m\omega t + n\omega_f t) \tag{3}$$

where ω is the eigen-frequency of the oscillation, which is unknown, and $a_{m,n}$, $b_{m,n}$ are constants, i.e., independent of time.

Based on the multi-scale method, two-time scales

$$\tau = \omega t, \quad \xi = \omega_f t \tag{4}$$

are introduced, we search for the solution expressed in the form

$$u(\tau) = \sum_{m=0}^{+\infty} \sum_{n=-\infty}^{+\infty} a_{m,n} \cos(m\tau + n\xi) + b_{m,n} \sin(m\tau + n\xi) \tag{5}$$

and the original (1) becomes

$$\omega^2 u_{\tau\tau} + 2\omega_f \omega u_{\tau\xi} + \omega_f^2 u_{\xi\xi} - \mu(1-u^2)(\omega u_\tau + \omega_f u_\xi) + \alpha u + \beta u^3 = g\cos(\xi) \quad (6)$$

subject to the boundary conditions

$$u = a, \quad \omega u_\tau + \omega_f u_\xi = 0, \quad when\ \tau = 0, \xi = 0 \quad (7)$$

We call (5) the solution expression.

Choose the auxiliary linear operator

$$\mathcal{L}u = u_{\tau\tau} + u_{\xi\xi} + u \quad (8)$$

with the properties

$$\mathcal{L}[\cos\tau] = 0, \quad \mathcal{L}[\cos\xi] = 0, \quad (9)$$

$$\mathcal{L}[\sin\tau] = 0, \quad \mathcal{L}[\sin\xi] = 0, \quad (10)$$

and

$$\mathcal{L}[\cos(m\tau \pm n\xi)] = [(1-(m^2+n^2))]\cos(m\tau \pm n\xi), \quad when\ m^2+n^2 > 1. \quad (11)$$

$$\mathcal{L}[\sin(m\tau \pm n\xi)] = [(1-(m^2+n^2))]\sin(m\tau \pm n\xi), \quad when\ m^2+n^2 > 1. \quad (12)$$

Therefore, the inverse operator reads

$$\mathcal{L}^{-1}[\cos(m\tau \pm n\xi)] = \frac{\cos(m\tau \pm n\xi)}{(1-(m^2+n^2))}, \quad when\ m^2+n^2 > 1. \quad (13)$$

$$\mathcal{L}^{-1}[\sin(m\tau \pm n\xi)] = \frac{\sin(m\tau \pm n\xi)}{(1-(m^2+n^2))}, \quad when\ m^2+n^2 > 1. \quad (14)$$

According to (6), a nonlinear operator is defined as

$$\begin{aligned}\mathcal{N}[U(\tau,\xi;q),\Omega(q)] = {} & \Omega^2(q)U_{\tau\tau}(\tau,\xi;q) + 2\omega_f\Omega(q)U_{\tau\xi}(\tau,\xi;q) \\ & +\omega_f^2 U_{\xi\xi}(\tau,\xi;q) \\ & -\mu[1-U^2(\tau,\xi;q)][\Omega(q)U_\tau(\tau,\xi;q) + \omega_f U_\xi(\tau,\xi;q)] \\ & +\alpha U(\tau,\xi;q) + \beta U^3(\tau,\xi;q) - g\cos(\xi) \end{aligned} \quad (15)$$

Let $q \in [0,1]$ denote the embedding parameter, $c_0 \neq 0$ an auxiliary parameter, $u_0(\tau,\xi)$, ω_0 and a_0 the initial approximations of the displacement, eigen-frequency, and amplitude of the oscillation, respectively. We construct a parameterized family of equation, namely the zeroth-order deformation equation, in the embedding parameter $q \in [0,1]$:

$$(1-q)\mathcal{L}[U(\tau,\xi;q) - u_0(\tau,\xi)] = qc_0\mathcal{N}[U(\tau,\xi;q),\Omega(q)] \quad (16)$$

subject to the boundary conditions

$$U(0,0;q) = A(q) \quad (17)$$

$$\Omega(q)U_\tau(\tau,\xi;q) + \omega_f U_\xi(\tau,\xi;q) = 0, \quad when\ \tau = 0, \xi = 0 \quad (18)$$

Obviously, when $q = 0$, (16), (17), and (18) have the solution

$$U(\tau,\xi;0) = u_0(\tau,\xi), \quad \Omega(0) = \omega_0, \quad A(0) = a_0 \quad (19)$$

When $q = 1$, (16), (17), and (18) are exactly the same as (6) and (7), provided

$$U(\tau, \xi; 1) = u(\tau, \xi), \quad \Omega(1) = \omega, \quad A(1) = a \tag{20}$$

Therefore, as the embedding parameter q increases from 0 to 1, the solution $U(\tau, \xi; q)$ varies from the initial guess $u_0(\tau, \xi)$ to the exact solution $u(\tau, \xi)$, so does $\Omega(q)$ from its initial guess ω_0 to the exact frequency ω, and $A(q)$ from its initial guess a_0 to the exact amplitude a of the limit cycles, respectively. For brevity, call (16), (17) and (18) the zeroth-order deformation equations.

From the Taylor's theorem, $U(\tau, \xi; q)$, $\Omega_i(q)$, and $A_i(q)$ are expanded in power series of q as follows:

$$U(\tau, \xi; q) = u_0(\tau, \xi) + \sum_{n=1}^{\infty} u_n(\tau, \xi) q^n, \tag{21}$$

$$\Omega_(q) = \omega_0 + \sum_{n=1}^{\infty} \omega_n q^n, \tag{22}$$

$$A_(q) = a_0 + \sum_{n=1}^{\infty} a_n q^n, \tag{23}$$

where

$$u_n(\tau, \xi) = \frac{1}{n!} \frac{\partial^n U(\tau, \xi; q)}{\partial q^n}\bigg|_{q=0}, \tag{24}$$

$$\omega_n = \frac{1}{n!} \frac{d^n \Omega_(q)}{dq^n}\bigg|_{q=0}, \tag{25}$$

$$a_n = \frac{1}{n!} \frac{d^n A(q)}{dq^n}\bigg|_{q=0}. \tag{26}$$

Assume that the value of c_0 is properly chosen that (21), (22), and (23) are convergent at $q = 1$. Then, due to (20), there holds

$$u_i(\tau, \xi) = u_0(\tau, \xi) + \sum_{n=1}^{\infty} u_n(\tau, \xi), \tag{27}$$

$$\omega = \omega_0 + \sum_{n=1}^{\infty} \omega_n, \tag{28}$$

$$a = a_0 + \sum_{n=1}^{\infty} a_n. \tag{29}$$

For the simplicity, three vectors are defined as

$$\mathbf{u}_n = \{u_0, u_1, u_2, \ldots, u_n\}, \tag{30}$$

$$\omega_n = \{\omega_0, \omega_1, \omega_2, \ldots, \omega_n\}, \tag{31}$$

$$\mathbf{a}_n = \{a_0, a_1, a_2, \ldots, a_n\}. \tag{32}$$

The results at the mth-order approximation are given by

$$u_i(\tau,\xi) = u_0(\tau,\xi) + \sum_{n=1}^{m} u_n(\tau,\xi), \tag{33}$$

$$\omega = \omega_0 + \sum_{n=1}^{m} \omega_n, \tag{34}$$

$$a = a_0 + \sum_{n=1}^{m} a_n. \tag{35}$$

Differentiating the zeroth-order deformation equation m times with respect to q, then dividing them by $m!$, and setting $q = 0$, we have the mth-order deformation equation as follows:

$$\mathcal{L}[u_m - \chi_m u_{m-1}] = c_0 \Delta_{m-1}(u_{m-1}, \omega_{m-1}, a_{m-1}) \tag{36}$$

subject to the boundary conditions

$$u_m(0,0) = a_m, \quad \sum_{i=0}^{m} \omega_i u_{m-i,\tau}(0,0) + \omega_f u_{m,\xi}(0,0) = 0. \tag{37}$$

where

$$\begin{aligned}\Delta_{m-1}(u_{m-1}, \omega_{m-1}) = {} & \sum_{i=0}^{m-1} u_{i,\tau\tau} \sum_{j=0}^{m-1-i} \omega_j \omega_{m-1-i-j} + 2\omega_f \sum_{i=0}^{m-1} \omega_i u_{m-1-i,\tau\xi} \\ & + \omega_f^2 u_{m-1,\xi\xi} - \mu\Big(\sum_{i=0}^{m-1} \omega_i u_{m-1-i,\tau} + \omega_f u_{m-1,\xi}\Big) \\ & + \mu\Big(\sum_{i=0}^{m-1} \omega_i \sum_{j=0}^{m-1-i} u_{j,\tau} \sum_{r=0}^{m-1-i-j} u_r u_{m-1-i-j-r} \\ & + \omega_f \sum_{i=0}^{m-1} u_{i,\xi} \sum_{j=0}^{m-1-i} u_j u_{m-1-i-j}\Big) + \alpha u_{m-1} \\ & + \beta \sum_{i=0}^{m-1} u_i \sum_{j=0}^{m-1-i} u_j u_{m-1-i-j} - (1-\chi_m) g\cos(\xi)\end{aligned} \tag{38}$$

and

$$\chi_m = \begin{cases} 0, m \le 1, \\ 1, m > 1. \end{cases} \tag{39}$$

Based on the solution from (5) and boundary conditions (37), we choose the initial guess

$$u_0(\tau,\xi) = (a_0 - B_0)\cos\tau + B_0\cos\xi + G_0\sin\tau - \frac{G_0\omega_0}{\omega_f}\sin\xi \tag{40}$$

where B_0 and G_0 are unknown constants. Thus, we have four unknown constants B_0, G_0, a_0, and ω_0 right now for the initial guess $u_0(\tau,\xi)$.

When $m = 1$,

$$\begin{aligned}\Delta_0(u_0, \omega_0) &= a_{1,0}\cos\tau + a_{0,1}\cos\xi + b_{1,0}\sin\tau + b_{0,1}\sin\xi \\ &\quad + \ldots \quad \ldots \end{aligned} \tag{41}$$

where

$$\begin{aligned} a_{1,0} &= a_0\alpha - \alpha B_0 + \frac{3a_0^3\beta}{4} - \frac{9}{4}a_0^2 B_0\beta + \frac{15}{4}a_0 B_0^2\beta - \frac{9B_0^3\beta}{4} + \frac{3}{4}a_0 G_0^2\beta \\ &\quad -\frac{3}{4}B_0 G_0^2\beta - G_0\mu\omega_0 + \frac{1}{4}a_0^2 G_0\mu\omega_0 - \frac{1}{2}a_0 B_0 G_0\mu\omega_0 + \frac{3}{4}B_0^2 G_0\mu\omega_0 \\ &\quad +\frac{1}{4}G_0^3\mu\omega_0 - a_0\omega_0^2 + B_0\omega_0^2 + \frac{3a_0 G_0^2\beta\omega_0^2}{2\omega_f^2} - \frac{3B_0 G_0^2\beta\omega_0^2}{2\omega_f^2} + \frac{G_0^3\mu\omega_0^3}{2\omega_f^2} \end{aligned} \tag{42}$$

$$\begin{aligned} a_{0,1} &= \alpha B_0 + \frac{3a_0^2 B_0\beta}{2} - 3a_0 B_0^2\beta + \frac{9B_0^3\beta}{4} + \frac{3}{2}B_0 G_0^2\beta - g \\ &\quad +G_0\mu\omega_0 - \frac{1}{2}a_0^2 G_0\mu\omega_0 + a_0 B_0 G_0\mu\omega_0 - \frac{3}{4}B_0^2 G_0\mu\omega_0 \\ &\quad -\frac{1}{2}G_0^3\mu\omega_0 + \frac{3B_0 G_0^2\beta\omega_0^2}{4\omega_f^2} - \frac{G_0^3\mu\omega_0^3}{4\omega_f^2} - B_0\omega_f^2 \end{aligned} \tag{43}$$

$$\begin{aligned} b_{1,0} &= \alpha G_0 + \frac{3a_0^2 G_0\beta}{4} - \frac{3}{2}a_0 B_0 G_0\beta + \frac{9}{4}B_0^2 G_0\beta + \frac{3G_0^3\beta}{4} + a_0\mu\omega_0 - \frac{1}{4}a_0^3\mu\omega_0 \\ &\quad -B_0\mu\omega_0 + \frac{3}{4}a_0^2 B_0\mu\omega_0 - \frac{5}{4}a_0 B_0^2\mu\omega_0 + \frac{3}{4}B_0^3\mu\omega_0 - \frac{1}{4}a_0 G_0^2\mu\omega_0 \\ &\quad +\frac{1}{4}B_0 G_0^2\mu\omega_0 - G_0\omega_0^2 + \frac{3G_0^3\beta\omega_0^2}{2\omega_f^2} - \frac{a_0 G_0^2\mu\omega_0^3}{2\omega_f^2} + \frac{B_0 G_0^2\mu\omega_0^3}{2\omega_f^2} \end{aligned} \tag{44}$$

$$\begin{aligned} b_{0,1} &= \frac{3G_0^3\beta\omega_0^3}{4\omega_f^3} - \frac{\alpha G_0\omega_0}{\omega_f} - \frac{3a_0^2 G_0\beta\omega_0}{2\omega_f} + \frac{3a_0 B_0 G_0\beta\omega_0}{\omega_f} \\ &\quad -\frac{9B_0^2 G_0\beta\omega_0}{4\omega_f} - \frac{3G_0^3\beta\omega_0}{2\omega_f} - \frac{B_0 G_0^2\mu\omega_0^2}{4\omega_f} + B_0\mu\omega_f \\ &\quad -\frac{1}{2}a_0^2 B_0\mu\omega_f + a_0 B_0^2\mu\omega_f - \frac{3}{4}B_0^3\mu\omega_f - \frac{1}{2}B_0 G_0^2\mu\omega_f + G_0\omega_0\omega_f \end{aligned} \tag{45}$$

Obviously, the term $\cos\tau$, $\cos\xi$, $\sin\tau$, and $\sin\xi$ of Δ_0 must disappear. Thus, we have to enforce

$$a_{1,0} = 0, \quad a_{0,1} = 0, \quad b_{1,0} = 0, \quad b_{0,1} = 0 \tag{46}$$

and B_0, G_0, a_0, and ω_0 can be determined by the system of nonlinear (46). Furthermore, we can have the first-order solution

$$u_1(\tau, \xi) = u_1^*(\tau, \xi) + B_1\cos\tau + G_1\cos\xi + C_1\sin\tau + D_1\sin\xi \tag{47}$$

where

$$u_1^*(\tau, \xi) = \mathcal{L}^{-1}[c_0\Delta_0] \tag{48}$$

B_1, G_1, C_1, D_1 are constants to be determined. Using the boundary conditions (37), we can determine the constants C_1 and D_1 which can be expressed by B_1 and G_1.

Thus, till now, only B_1, G_1, a_1, and ω_1 are unknown. They can be determined by avoiding the secular terms $\cos\tau, \cos\xi, \sin\tau$, and $\sin\xi$ in Δ_1 when $m = 2$.

Similarly, when $m > 1$, we can have the mth-order approximation

$$u_m(\tau,\xi) = \chi_m u_{m-1}(\tau,\xi) + u_m^*(\tau,\xi) + B_m\cos\tau + G_m\cos\xi + C_m\sin\tau + D_m\sin\xi \tag{49}$$

where

$$u_m^*(\tau,\xi) = \mathcal{L}^{-1}[c_0\Delta_{m-1}] \tag{50}$$

C_m and D_m can be also expressed by B_m and G_m according to the boundary conditions (37), and B_m, G_m, a_m, and ω_m can be determined by avoiding the four secular terms $\cos\tau, \cos\xi, \sin\tau$, and $\sin\xi$ in Δ_m in the next order $m+1$.

In order to choose a proper value of c_0, the squared residual error is defined

$$\mathcal{E}_i(c_0) = \int_0^{2\pi} (\mathcal{N}[u(t),\omega,a])^2 dt. \tag{51}$$

For the sake of computational efficiency, the squared residual error $\mathcal{E}_i$ is calculated numerically,

$$\mathcal{E}_i(c_0) \approx \bar{\mathcal{E}}_i(c_0) = \frac{1}{N+1}\sum_{k=0}^{N}\left(\mathcal{N}[u(t),\omega,a]\Big|_{t=k\Delta t}\right)^2, \tag{52}$$

where $\Delta t = 2\pi/N$ and N is an integer. Obviously, the above expression is a good approximation of $\mathcal{E}_i$ for large enough N. In this paper, $N = 50$. Given the initial guess $u_0(\tau,\xi)$ and the auxiliary linear operator $\mathcal{L}$, the discrete squared residual error $\bar{\mathcal{E}}_i$ is only dependent on the convergence-control parameters c_0, whose optimal value are determined by the minimum of $\bar{\mathcal{E}}_i$. Thus, unlike other analytic methods, the HAM

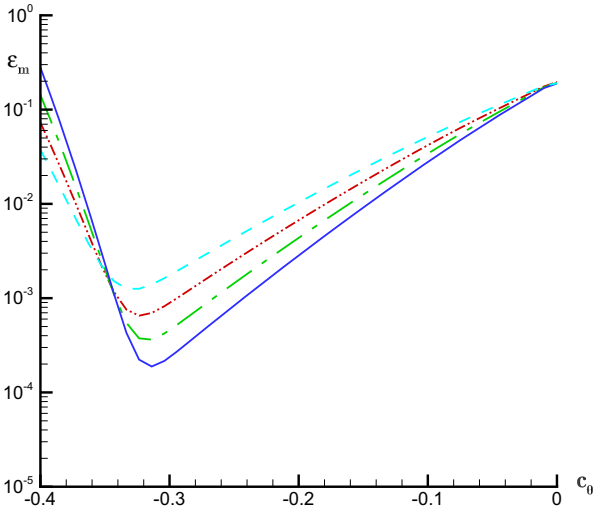

Fig. 2 Discrete square residual $\bar{\mathcal{E}}_m(c_0)$ in the case of $\mu = \frac{1}{10}, \beta = 0, \alpha = 1, g = \frac{1}{2}, w_f = 2$ by the corresponding optimal convergence-control parameter $c_0 = -\frac{31}{100}$. Dashed: second-order approx.; DashDotDot: third-order approx.; DashDot: fourth-order approx.; solid: fifth-order approx

Table 1 The discrete square residual $\bar{\mathcal{E}}_m(c_0)$ in the case of $\mu = \frac{1}{10}, \beta = 0, \alpha = 1, g = \frac{1}{2}, w_f = 2$ by the optimal convergence-control parameter $c_0 = -\frac{31}{100}$

m, order of approx.	$\bar{\mathcal{E}}_m(c_0)$
1	$8.5935960940 \times 10^{-3}$
5	$4.5603847951 \times 10^{-4}$
10	$1.2306233210 \times 10^{-5}$
15	$8.3085442636 \times 10^{-7}$
25	$4.1182799933 \times 10^{-8}$
35	$6.5870508257 \times 10^{-9}$
45	$2.2182312610 \times 10^{-9}$

provides a convenient way to guarantee the convergence of the series solution [17–19].

3 Results and discussions

Being different from the research on limit cycle (A *limit cycle* is a closed trajectory in phase space having the property that at least one other trajectory spirals into it either as time approaches infinity or as time approaches negative infinity.) analytically, and due to the specific natures of the analytic period-doubling and quasi-periodic solutions, here,

$$\delta = \left| 1 - \frac{u_A(t)}{u_N(t)} \right|, \quad at \;\; t = T_c \tag{53}$$

is defined as the relative error between the approximation solution $u_A(t)$ obtained by the HAM and the numerical result $u_N(t)$ based on the classical Runge-Kutta method at $t = T_c$. The critical predictable time T_c can be interpreted as follows: in this paper, If $\delta \leq 5\%$ with $t \in [0, T_c]$, the approximation solution $u_A(t)$ obtained by the HAM can be regarded as a reliable solution in this interval, and this thought comes from the reference [20].

Without loss of generality, four sets of parameters are considered.

Case A: $\mu = \frac{1}{10}, \beta = 0, \alpha = 1, g = \frac{1}{2}, w_f = 2$.

To illustrate the convergence of the HAM series solutions, take *Case A* for example. As shown in Fig. 2, as the order of the approximation increases, the discrete

Table 2 The homotopy-approximations of a and ω in the case of $\mu = \frac{1}{10}, \beta = 0, \alpha = 1, g = \frac{1}{2}, w_f = 2$ by the corresponding optimal convergence-control parameter $c_0 = -\frac{31}{100}$

m, order of approx.	a	ω
1	1.820044340	1.0000000006
5	1.820550645	0.9995121219
10	1.820666931	0.9993961369
15	1.820668447	0.9993781088
25	1.820747199	0.9993750589
35	1.820791789	0.9993754377
45	1.820829612	0.9993763969

Table 3 Some reliable analytical results with $T_c = 5000$ in the case of $\mu = \frac{1}{10}, \beta = 0, \alpha = 1, g = \frac{1}{2}, w_f = 2$ by the corresponding optimal convergence-control parameter $c_0 = -\frac{31}{100}$

t	$u_A(t)$	$u_N(t)$	δ
1	1.176972694	1.176925098	0.0003582
10	− 1.723625232	− 1.723718957	0.0001467
50	− 1.723625232	− 1.723718957	0.0000423
100	1.556751053	1.555898745	0.0012903
200	0.780312984	0.777208179	0.0039948
300	− 0.304700044	− 0.308961871	0.0137940
400	− 1.355048605	− 1.358525291	0.0025591
500	− 2.029290522	− 2.030462598	0.0005772
700	− 1.100541325	− 1.096100216	0.0040517
800	0.224965891	0.229240046	0.0186448
900	1.351923422	1.354484347	0.0018907
1000	1.931655204	1.932353798	0.0033908
1200	1.145321548	1.145841490	0.0004537
1500	− 1.554417652	− 1.551924094	0.0016067
1800	− 0.726270454	− 0.732364983	0.0083217
2000	1.634806032	1.631674517	0.0010515
2200	1.807411244	1.808431322	0.0005640
2500	− 1.328462313	− 1.330520749	0.0015470
2800	− 1.173006129	− 1.167041802	0.0051106
3000	0.876259451	0.883368669	0.0080450
3200	2.101633183	2.100801885	0.0003957
3500	− 0.864316410	− 0.868906641	0.0045902
3600	− 1.753032520	− 1.755097348	0.0011764
3800	− 1.543589168	− 1.542930153	0.0004271
3900	− 0.616869693	− 0.617278998	0.0006630
4000	0.399889370	0.398159951	0.0043435
4300	1.853640173	1.854826575	0.0006396
4500	0.070017086	0.072109241	0.0290136
4700	− 1.981375640	− 1.981419598	0.0000221
4800	− 2.086019161	− 2.085518820	0.0002399
4900	− 1.344164941	− 1.341266737	0.0021607
4950	− 0.754178584	− 0.749844658	0.0057797
4990	− 0.694699650	− 0.699539376	0.0069184
5000	− 0.126025672	− 0.120530688	0.0455899

squared residual $\bar{\mathcal{E}}_m(c_0)$ decreases in the region $R_c = \{c_0 | -\frac{9}{25} \leq c_0 \leq 0\}$. When $\frac{d\mathcal{E}_5(c_0)}{dc_0} = 0$, the optimal convergence-control parameter c_0 is chosen as $c_0 = -\frac{31}{100}$. It is found that, as the order of the approximation increases, the discrete squared

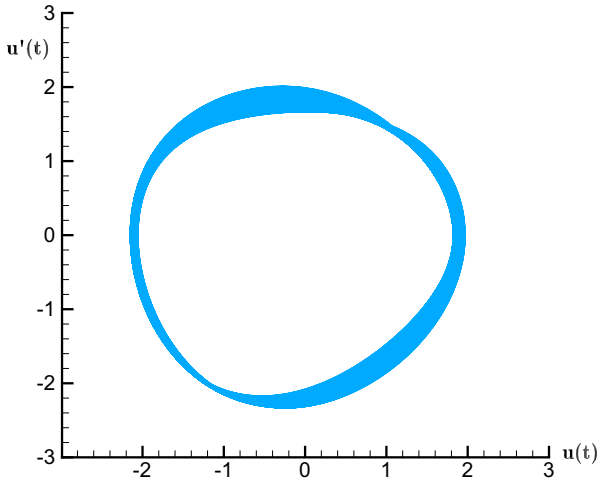

Fig. 3 The $u - \dot{u}$ plane projection of the quasi-periodic solutions given by the reliable quasi-periodic solutions with $T_c = 1000$ in the case of $\mu = \frac{1}{10}, \beta = 0, \alpha = 1, g = \frac{1}{2}, w_f = 2$ by the corresponding optimal convergence-control parameter $c_0 = -\frac{31}{100}$

residuals of all these homotopy-series decrease monotonously. All the HAM series solutions are expanded to the 45th order with residual error less than 5×10^{-9}, as shown in Table 1. Table 2 shows that the amplitude a and the frequency ω converge to the values 1.8208 and 0.999376, respectively, as the order of the approximation m increases to 45. As shown in the left-hand chart of the Fig. 5, the analytic solutions obtained in the case of $\mu = \frac{1}{10}, \beta = 0, \alpha = 1, g = \frac{1}{2}, w_f = 2$ by mean of $c_0 = -\frac{31}{100}$ are quasi-periodic. And as seen from the Table 3, the HAM series solutions are proved effective even when $t = 5000$ by comparing with numerical results, and this means that T_c is 5000 at least. Also, the $u - \dot{u}$ plane projections of the quasi-periodic solutions given by the $35th$-order approximation in different time intervals and the $u - \dot{u}$ plane projections of the quasi-periodic solutions when $T_c \in [0, 200]$ with this set of parameters compared with the numerical results based on a fourth-order Runge-Kutta method are plotted in Fig. 5. It is worth noting that the numerical results obtained by the fourth-order Runge-Kutta method agree closely with the series solution for *Case A*, as shown in Figs. 3 and 4 even when only $T_c = 1000$ and $T_c = 3000$, respectively.

Case B: $\mu = \frac{1}{10}, \beta = 0, \alpha = 1, g = \frac{1}{2}, w_f = \frac{19}{10}$.

Compared with *Case A*, in addition to the small change of the value of w_f, the values of the other parameters remain unchanged. Similarly, the optimal convergence-control parameter c_0 is chosen as $c_0 = -\frac{1}{5}$ and all the HAM series solutions are expanded to the 23th order with residual error less than 5×10^{-6}. The amplitude a and the frequency ω converge to the values 1.79121 and 0.999361, respectively, as the order of the approximation m increases to 23. The $u - \dot{u}$ plane projection of the quasi-periodic solutions given by the $23th$-order approximation in different time intervals and comparison of the $u - \dot{u}$ plane projection of the quasi-periodic solutions

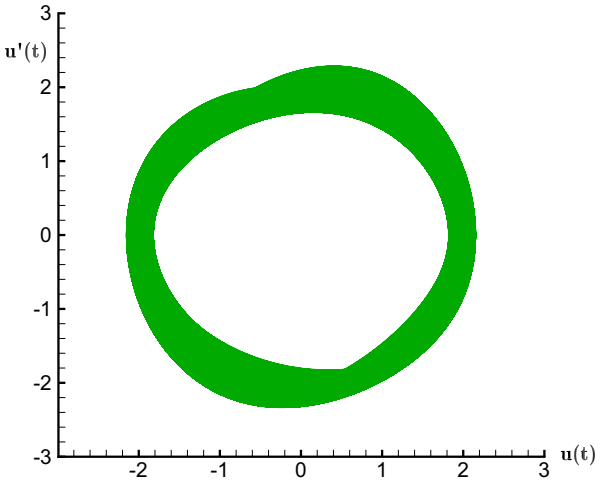

Fig. 4 The $u - \dot{u}$ plane projection of the quasi-periodic solutions given by the reliable quasi-periodic solutions with $T_c = 3000$ in the case of $\mu = \frac{1}{10}, \beta = 0, \alpha = 1, g = \frac{1}{2}, w_f = 2$ by the corresponding optimal convergence-control parameter $c_0 = -\frac{31}{100}$

with the numerical results when $T_c \in [0, 100]$ in the case of $\mu = \frac{1}{10}, \beta = 0, \alpha = 1, g = \frac{1}{2}, w_f = \frac{19}{10}$ by mean of $c_0 = -\frac{1}{5}$ are shown in Fig. 6. However, it can be easily found that the right-hand chart of Fig. 6 is more complex than the right-hand chart of Fig. 5, although the difference of w_f only is 0.1. It can be concluded from the discussion that understanding of nonlinear oscillatory systems analytically is a heavy-burden and long-way arduous task. Thereinto, $T_c = 2000$ is also obtained by the (53) easily.

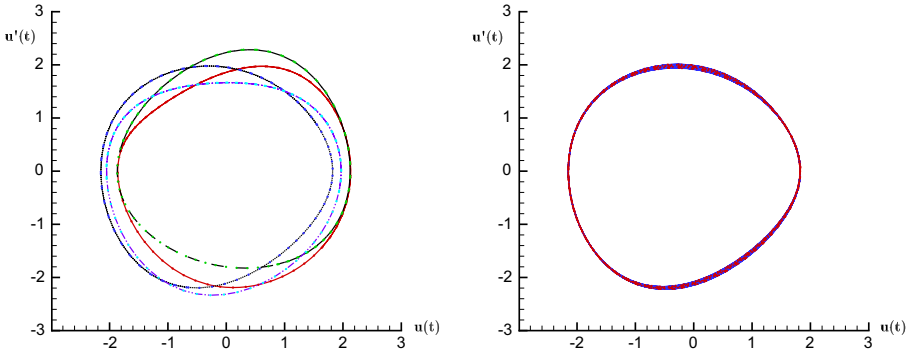

Fig. 5 (Left): The $u - \dot{u}$ plane projection of the quasi-periodic solutions given by the $35th$-order approximation in case of $\mu = \frac{1}{10}, \beta = 0, \alpha = 1, g = \frac{1}{2}, w_f = 2$ by mean of $c_0 = -\frac{31}{100}$ in different time intervals. Dotted: $t \in [90, 100]$, DashDotDot: $t \in [990, 1000]$, dashed: $t \in [1990, 2000]$, solid: $t \in [2990, 3000]$; (right): comparison of the $u - \dot{u}$ plane projection of the quasi-periodic solutions with the numerical results when $T_c \in [0, 200]$, solid line: the $35th$-order approximation by mean of $c_0 = -\frac{31}{100}$, filled circle: numerical results

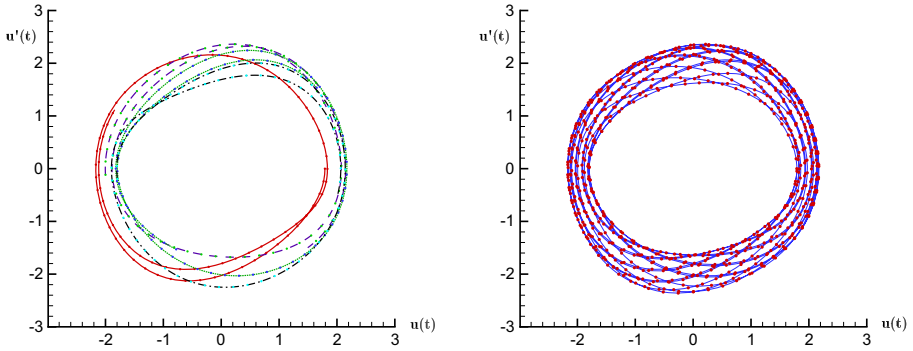

Fig. 6 (Left): The $u - \dot{u}$ plane projection of the quasi-periodic solutions given by the $23th$-order approximation in the case of $\mu = \frac{1}{10}, \beta = 0, \alpha = 1, g = \frac{1}{2}, w_f = \frac{19}{10}$ by mean of $c_0 = -\frac{1}{5}$ in different time intervals. DashDot: $t \in [0, 10]$, Dotted: $t \in [90, 100]$, Solid: $t \in [990, 1000]$, Dashed: $t \in [1990, 2000]$; (Right): Comparison of the $u - \dot{u}$ plane projection of the quasi-periodic solutions with the numerical results when $T_c \in [0, 100]$, Solid line: the $23th$-order approximation by mean of $c_0 = -\frac{1}{5}$, Filled circle: Numerical resultsx

Case C: $\mu = \frac{1}{10}, \beta = 1, \alpha = 1, g = \frac{1}{1000}, w_f = 2$.

Compared with *Case A* and *Case B*, the previous two cases are the forced Van der Pol oscillators ($\beta = 0$). However, *Case C* is used to describe the forced Van der Pol-Duffing oscillator ($\beta \neq 0$). Because of the small value of $g = \frac{1}{1000}$, the forced oscillation is equivalent to free oscillation approximatively. Similarly, the optimal convergence-control parameter c_0 is chosen as $c_0 = -\frac{1}{5}$ and all the HAM series solutions are expanded to the $10th$ order with residual error less than 1×10^{-6}. The amplitude a and the frequency ω converge to the values 1.93455 and 1.92862, respectively, as the order of the approximation m increases to 10. The $u - \dot{u}$ plane projection of the limit cycles given by the $10th$-order approximation in different time

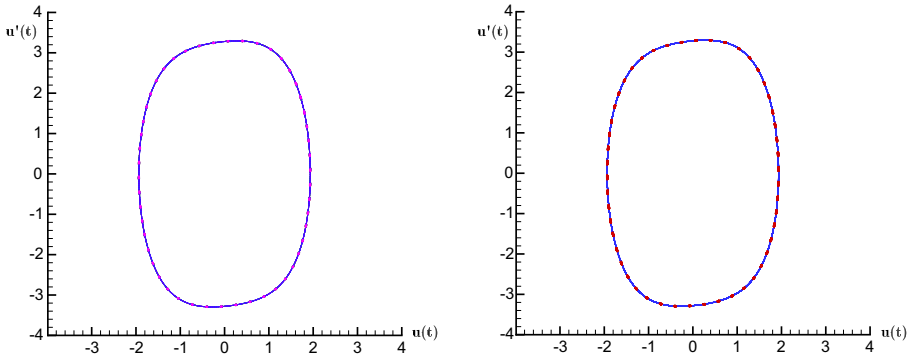

Fig. 7 (Left): The $u - \dot{u}$ plane projection of the limit cycles given by the $10th$-order approximation in case of $\mu = \frac{1}{10}, \beta = 1, \alpha = 1, g = \frac{1}{1000}, w_f = 2$ by mean of $c_0 = -\frac{1}{5}$ in different time intervals. DashDot: $t \in [0, 10]$, Dotted: $t \in [90, 100]$, Solid: $t \in [990, 1000]$, Dashed: $t \in [1990, 2000]$; (Right): Comparison of the $u - \dot{u}$ plane projection of the limit cycle with the numerical results when $T_c \in [0, 200]$, Solid line: the $10th$-order approximation by mean of $c_0 = -\frac{1}{5}$, Filled circle: Numerical results

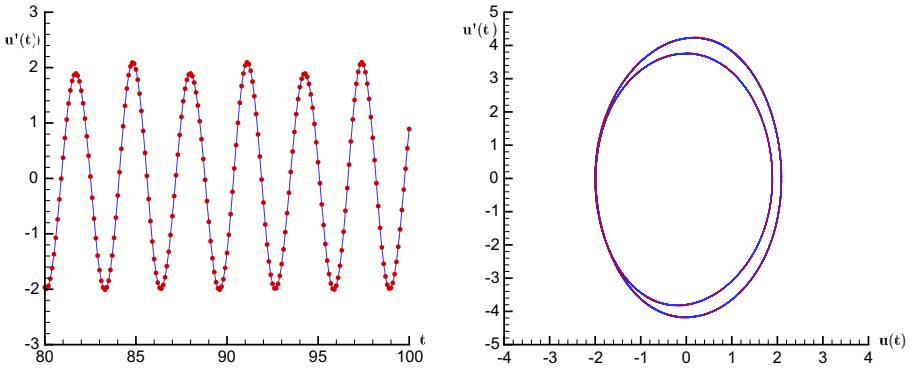

Fig. 8 (Left): Comparison of the $u(t)$ given by the $8th$-order approximation in the case of $\mu = \frac{1}{10}, \beta = 0, \alpha = 4, g = \frac{1}{2}, w_f = 3$ with the numerical results when $T_c \in [80, 100]$, solid line: the $8th$-order approximation by mean of $c_0 = -\frac{1}{10}$, filled circle: numerical results; (right): Comparison of the $u - \dot{u}$ plane projection of the period-doubling solutions with the numerical results when $T_c \in [0, 100]$, solid line: the $8th$-order approximation by mean of $c_0 = -\frac{1}{10}$, filled circle: numerical results

intervals and comparison of the $u - \dot{u}$ plane projection of the limit cycle with the numerical results when $T_c \in [0, 200]$ in the case of $\mu = \frac{1}{10}, \beta = 1, \alpha = 1, g = \frac{1}{1000}, w_f = 2$ by mean of $c_0 = -\frac{1}{5}$ are shown in Fig. 7. Obviously, the HAM series solutions obtained are limit cycles, as shown in the left-hand chart of Fig. 7. Also, $T_c = 2000$ can be obtained by the (53) easily.

Case D: $\mu = \frac{1}{10}, \beta = 0, \alpha = 4, g = \frac{1}{2}, w_f = 3$.

Same with *Case A* and *Case B*, this case also is the forced Van der Pol oscillators ($\beta = 0$). Similarly, the optimal convergence-control parameter c_0 is chosen as $c_0 = -\frac{1}{10}$ and all the HAM series solutions are expanded to the $8th$ order with residual error less than 5×10^{-4}. The amplitude a and the frequency ω converge to the values 1.8952 and 1.99969, respectively, as the order of the approximation m increases to 8. Comparison of the $u(t)$ given by the $8th$-order approximation with the numerical results when $T_c \in [80, 100]$ and comparison of the $u - \dot{u}$ plane projection of the period-doubling solutions in the case of $\mu = \frac{1}{10}, \beta = 0, \alpha = 4, g = \frac{1}{2}, w_f = 3$ by mean of $c_0 = -\frac{1}{10}$ with the numerical results when $T_c \in [0, 100]$ are plotted in Fig. 8. Obviously, the HAM series solutions obtained are period-doubling, as shown in the right-hand chart of Fig. 8. Also, $T_c = 100$ can be obtained by the (53) easily.

4 Conclusions

An approximate analytic method that combines the homotopy analysis method (HAM) with the multi-scale method is proposed to study the limit cycles, period-doubling, and quasi-periodic solutions of the forced Van der Pol oscillator and the forced Van der Pol-Duffing oscillator. The accuracy and efficiency of the proposed method have been demonstrated by the numerical results. This approach has general meanings and thus can be used to solve many same types of highly nonlinear oscillating systems in science and engineering.

Acknowledgements The authors gratefully acknowledge the financial support from the Science Research Project of Inner Mongolia University of Technology (Approval No. ZD201613) and the science research project of Huazhong University of Science and Technology (Approval No. 0118140077 and 2006140115). This work was partly supported by the National Natural Science Foundation of China (NSFC) under Project Nos. 51609090 and 51679097.

Author Contributions All authors contributed equally to the writing of this paper. All authors read and approved the final manuscript.

Compliance with Ethical Standards

Competing interests The authors declare that they have no competing interests.

References

1. Lazer, A.C., McKenna, P.J.: Large-amplitude periodic oscillations in suspension bridges: some new connections with nonlinear analysis. SIAM Rev. **32**(4), 537–578 (1990)
2. Kaplan, D., Glass, L.: Understanding Nonlinear Dynamics. Springer, New York (1995)
3. Richard, H.: It's a Nonlinear World. Springer, New York (2011)
4. Pranay, P., Dhiman, M., Andreas, A., Saibal, R.: Influence of combined fundamental potentials in a nonlinear vibration energy harvester. Sci. Rep. **6**, 1–13 (2016)
5. FitzHugh, R.: Impulses and physiological states in theoretical models of nerve membranes. Biophys. **1**, 445–466 (1961)
6. Nagumo, J., Arimoto, S., Yoshizawa, S.: An active pulse transmission line simulating nerve axon. Proc. IEEE **50**, 2061–2070 (1962)
7. Cartwright, J., Eguiluz, V., Hernandez-Garcia, E., Piro, O.: Dynamics of elastic excitable media. Int. J. Bifurc. Chaos **9**, 2197–2202 (1999)
8. Lucero, J.C., Schoentgen, J.: Modeling vocal fold asymmetries with coupled van der Pol oscillators. Proc. Meetings Acoustics **19**(1), 060165 (2013)
9. Cui, J.F., Liang, J.M., Lin, Z.L.: Stability analysis for periodic solutions of the Van der Pol-Duffing forced oscillator. Phys. Scripta **91**(1), 7pp (2015)
10. Shukla, A.K., Ramamohan, T.R., Srinivas, S.: Analytical solutions for limit cycles of the forced Van der Pol-Duffing oscillator. AIP Conf. Proc. **1558**, 2187–2192 (2013)
11. Stupnicka, W.S.: The coexistence of periodic, almost periodic and chaotic attractors in the Van der Pol-Duffing oscillator. J. Sound Vib. **199**(2), 165–175 (1997)
12. Shukla, A.K., Ramamohan, T.R., Srinivas, S.: A new analytical approach for limit cycles and quasi-periodic solutions of nonlinear oscillators: the example of the forced Van der Pol-Duffing oscillator. J. Sound Vib. **89**, 10pp (2014)
13. Chen, Y.M., Liu, J.K.: A study of homotopy analysis method for limit cycle of Van der Pol equation. Commun. Nonlinear Sci. Numer. Simul. **14**(5), 1816–1821 (2009)
14. Chen, Y.M., Liu, J.K.: Uniformly valid solution of limit cycle of the Duffing-van der Pol equation. Mech. Res. Commun. **36**, 845–850 (2009)
15. Kimiaeifar, A., Saidi, A.R., Bagheri, G.H., Rahimpour, M.D., Domairry, G.: Analytical solution for Van der Pol-Duffing oscillators. Chaos Soliton Fract. **42**, 2660–2666 (2009)
16. Kartashova, E.: Nonlinear Resonance Analysis: Theory, Computation, Applications. Cambrige University Press, Cambrige (2011)
17. Liao, S.J.: An optimal homotopy-analysis approach for strongly nonlinear differential equations. Commun. Nonlinear Sci. Numer. Simul. **15**(8), 2003–2016 (2010)
18. Liao, S.J.: Homotopy Analysis Method in Nonlinear Differential Equations. Higher Education Press, Beijing (2012)
19. Liao, S.J.: Advances in the Homotopy Analysis Method. World Scientific, New York (2013)
20. Liao, S.J.: On the reliability of computed chaotic solutions of non-linear differential equations. Tellus **6IA**, 550–564 (2009)